Poly(methyl methacrylate) Grafting onto Stainless Steel Surfaces: Application to Drug-Eluting Stents

Yulia Shaulov,[†] Regina Okner,[†,‡] Yair Levi,[†] Noam Tal,[†] Vitaly Gutkin,[§] Daniel Mandler,[‡] and Abraham J. Domb*[,†]

Institute of Chemistry, Hebrew University of Jerusalem, Jerusalem 91904, Israel, Department of Medicinal Chemistry and Natural Products, School of Pharmacy, Faculty of Medicine, Hebrew University of Jerusalem, Jerusalem 91120, Israel, and Unit for Nanoscopic Characterization, Harwey Kreuger Family Center for Nanoscience and Nanotechnology of the Hebrew University of Jerusalem, Jerusalem 91904, Israel

ABSTRACT Drug-eluting stents (DESs) have been associated with adverse clinical effects. Moreover, recent publications have shown that the coating of DESs suffers from defects. The purpose of this contribution is to examine a three-step process for surface modification as a means of improving the durability of DESs. In the first step, 4-(2-bromoethyl)benzenediazonium tetrafluoroborate was electrografted onto a stainless steel (SS) stent. X-ray photoelectron spectroscopy (XPS) of the modified stent confirmed the formation of the organic layer. In the second step, methyl methacrylate was polymerized onto the grafted surface by atom-transfer radical polymerization. XPS, electrochemical impedance spectroscopy, and contact-angle measurements were used to characterize the polymer brushes. The last step involved spray-coating of the stent with a drug-in-polymer matrix [poly(*n*-butyl methacrylate)/poly(ethylene-*co*-vinyl acetate) + paclitaxel]. Scanning electron microscopy confirmed the considerably improved durability of the drug-in-polymer matrix. Bare controls showed greater cracking and delamination of the coating than did the two-step modified stents after incubation under physiological (37 °C) and accelerated (60 °C) conditions. Finally, paclitaxel controlled release from the modified SS DESs was moderate compared with that of nontreated samples. In conclusion, the proposed method significantly improves the durability of drug-in-polymer matrixes on a SS DESs.

KEYWORDS: diazonium salt • drug-eluting stent • electrocoating • PMMA grafting

1. INTRODUCTION

Drug-eluting stents (DESs) are designed to release an antirestenotic agent. During their preparation, the metallic scaffold is coated with a functional layer that releases the drug intended to block cell proliferation, and thereby prevent the reocclusion of the artery (restenosis) (1, 2). Two intensively investigated and FDA-approved DESs are the Sirolimus−Cypher stent (by Cordis), which elutes rapamycin (3), and Taxus (by Boston Scientific), which elutes paclitaxel (4). In both DESs, the backbone is made of stainless steel (SS), and nonbiodegradable polymers are used as drug carriers.

Stents are manufactured using various metallic alloys, including cobalt chromium (CoCr) (5), nitinol (6), and SS (1, 7). The surfaces of SS stents are usually coated with an oxide layer (10−50 Å) and hydroxides (8, 9). The oxide layer is fragile and mechanically unstable under stress conditions. Its chemical composition can also be altered with exposure to physiological environments (8, 10). Therefore, the common approach is to modify the metallic stent surface to enhance its biocompatibility. For example, coating the stent with iridium oxide or diamondlike carbon layers was investigated as a means of blocking the diffusion of toxic metallic ions such as nickel, chromate, and molybdenum (7, 8) into living tissues.

To improve the biocompatibility of DESs, hemocompatible coatings were applied, such as heparin- (11) and phosphorylcholine-based (12, 13) polymers (because of their nonthrombogenic characteristics). In general, the backbones of DESs are coated with either a biostable (2, 4, 7, 14) or biodegradable polymeric matrix (15, 16) that encapsulates the drug. The polymeric matrix allows loading of different drugs/agents and doses, resulting in diverse physicochemical properties of the DES. The durability of the drug-in-polymer matrix is crucial because the stent is a permanent implant that goes through various mechanical constraints, including crimping, delivery (implantation), and balloon inflation.

DESs were found to be superior to bare stents in clinical trials and implantations (17, 18). However, in the past few years, because of the adverse clinical effects (e.g., late-stage thrombosis) of some commercially available DESs, the long-term safety of DESs has been questioned (19−21). Moreover, recent publications revealed findings of defects in the coating of the commercial DESs (22).

* Corresponding author. E-mail: avid@ekmd.huji.ac.il. Tel: +972-2-6757573. Fax: +972-2-6757629.

Received for review July 11, 2009 and accepted September 23, 2009

[†] Department of Medicinal Chemistry and Natural Products, School of Pharmacy, Faculty of Medicine, Hebrew University of Jerusalem.

[‡] Institute of Chemistry, Hebrew University of Jerusalem.

[§] Harwey Kreuger Family Center for Nanoscience and Nanotechnology of the Hebrew University of Jerusalem.

DOI: 10.1021/am900465t

A possible method for improving the durability and adhesion of drug-in-polymer coatings of SS surfaces involves modification of the stent surface by the covalent attachment of organic species. It is known that aromatic diazonium (phenyldiazonium) salts can be electrochemically reduced to form a covalent bond with conducting surfaces. Phenyldiazonium and its para-substituted derivatives have been successfully electrografted onto carbon (23, 24), semiconductors (23), and diverse metals (23−28), but until now, only a few studies have examined the electrografting of diazonium salts onto SS surfaces (29).

Aromatic diazonium molecules can support various functionalities and initiate further polymerization. The "grafting from" method involves the covalent immobilization of small initiator molecules onto a surface (producing high-density initiators on the surface) followed by subsequent polymerization (30).

In recent years, there has been extensive investigation of the grafting of styrene, methacrylate, and acrylate monomers onto multiwalled carbon nanotubes (24), gold (30), and iron (31, 32) using atom-transfer radical polymerization (ATRP). Poly(methyl methacrylate) (PMMA) is a biocompatible polymer widely used in bone cements (33), load-bearing applications, and medical devices (34). The formation of PMMA brushes using a brominated aryldiazonium salt has been demonstrated on iron disks (24, 31). Although not part of this work, covalently bound PMMA polymer brushes on stent surfaces may enhance the durability of drug-in-polymer matrixes; still, its hemocompatibility should be determined. Recent publications have demonstrated the effectiveness of electrografting 4-(1-dodecyloxy)phenyldiazonium tetrafluoroborate ($C_{12}H_{25}O$-phenyldiazonium) onto both CoCr and SS stents and that the ultrathin layers that were formed enhanced the durability of various drug-in-polymer matrixes (29).

We examined a three-step coating process to enhance the durability of the drug-in-polymer matrix on a SS stent. In the first step, 4-(2-bromoethyl)benzenediazonium tetrafluoroborate (BrD) was electrochemically reduced on a SS stent, forming a carbon−metal covalent bond. X-ray photoelectron spectroscopy (XPS) and electrochemical impedance spectroscopy (EIS) of the BrD-modified stent were used to study the formation of the thin organic layer. In the second step, BrD-derived coating was used to initiate ATRP of methyl methacrylate (MMA). The PMMA brushes on the SS surface were characterized using XPS, EIS, and contact-angle measurements. The last step involved spray coating of the modified stents with a drug-in-polymer matrix [poly(*n*-butyl methacrylate) (PBMA)/poly(ethylene-*co*-vinyl acetate) (PEVA) + paclitaxel]. The durability of the drug-in-polymer matrix was visualized by scanning electron microscopy (SEM). Paclitaxel controlled release was tested for 3 weeks using high-pressure liquid chromatography (HPLC).

2. EXPERIMENTAL SECTION

2.1. Materials. 316 L stainless steel (SS) stents (Classic Infinite-1 design, with a length of 9 mm, a surface area of ca. 49 mm^2, and a closed diameter of 1.4 mm) and 316 L SS plates (10 × 30 mm^2) were obtained from STI Laser Industries, Ltd., Israel. SS plates were used for contact-angle and EIS measurements of the modified surfaces, and 316 L SS stents were used for EIS measurements, XPS analysis, durability studies, and in vitro drug release.

Tetrabutylammonium tetrafluoroborate (Bu_4NF_4B), CuCl, $CuCl_2$, *N*,*N*,*N*′,*N*″,*N*″-pentamethyldiethylenetriamine (PMDETA), 1-phenylethyl bromide (1-PhEtBr), poly(*n*-butyl methacrylate) (PBMA; molecular weight 340 000 Da; polydispersity 2.58), and methyl methacrylate (MMA) were obtained from Sigma-Aldrich, Israel. Sodium dodecyl sulfate (SDS), disodium hydrogen phosphate dodecahydrate, and sodium dihydrogen phosphate monohydrate were received from Reidel-de Haën, Germany. Poly(ethylene-*co*-vinyl acetate) (PEVA; molecular weight 116 467 Da; polydispersity 3.1) was obtained from DuPont, USA. Paclitaxel was obtained from Bioxefarma, Canada. All aqueous solutions were prepared using double-distilled water (DDW; Barnstead Easypure UV system, USA). Organic solvents were all analytical grade and purchased from Biolab, Israel. Acetonitrile was ultradry (ACN, 5−10 ppm of H_2O). Solvents used for the coating and treatment of the SS surfaces were purged with nitrogen before use.

2.2. Methods. 2.2.1. ***4-(2-Bromoethyl)benzenediazonium Tetrafluoroborate (BrD) Synthesis.*** The diazonium salt BrD was synthesized in a process described previously (24, 31). In the first step, the free amine bromide was prepared from commercially available 2-(4-aminophenyl)ethanol. In the second step, crystalline diazonium salt ($C_8H_8N_2BrBF_4$) was obtained by diazotation of the bromoethenylaniline. ^{1}H NMR and Fourier transform IR (FTIR) analyses were used to confirm the chemical structure of the product.

^{1}H NMR (D_2O): δ 8.30 (d, J = 9.0 Hz, 2H, C*H*-β), 7.66 (d, J = 8.7 Hz, 2H, C*H*-α), 3.59 (t, J = 6.6 Hz, 2H, CH_2Br), 3.28 (t, J = 6.6 Hz, 2H, ArCH_2).

FTIR: 3005−3097 (CH_2, C−H), 2254 ([RC═N═N^+] diazonium salt), 1627−1399 (C−C, aromatic ring), 1081 (aromatic ring in-plane C−H vibrations), 633 (C−Br).

2.2.2. ***Electrocoating of BrD.*** Electrochemical measurements were conducted with a 630B electrochemical analyzer (CH Instruments, Austin, TX, USA) using a three-electrode cell, with Ag/AgBr (or a Pt wire) as the reference electrode and a Pt wire as the counter electrode. The working electrodes were either 316 L SS plates or stents. The 316 L SS plates were treated with 2000 grit emery paper (Buehler Ltd., Lake Bluff, IL), followed by gentle polishing with 1 and 0.05 μm alumina paste suspensions. Cleaned plates and stents were washed in an ultrasonic bath with DDW and ACN (15 min for each solvent) and dried with a gentle stream of nitrogen.

To expose the elemental metal, mostly iron, the SS plates were electrochemically reduced at −2.5 V vs Pt for 30 min in a deaerated and dry 0.1 M TBATFB/ACN solution (35). Next, 1 mL of dry ACN with BrD was injected to produce a final concentration of 8 mM. A potential sweep was applied (30 cycles) between 0 and −1.6 V vs Pt at a scan rate of 100 mV/s. The electrochemical conditions for the SS stents were similar to those of the plates, but a potential of −1.6 V was applied (for 15 min) during cathodic pretreatment. Finally, the coated samples (abbreviated as BrD stents; Scheme 1) were immersed in an ultrasonic bath with ACN for 15 min to remove the excess of unbound material and dried with a gentle steam of nitrogen. The blocking characteristics of the modified surfaces were examined by cycling the potential from −0.4 to 1.2 V vs Ag/AgBr in the presence of 1 mM ferrocene (Fc) and 0.1 M TBATFB, before and after BrD grafting.

2.2.3. ***Surface-Initiated ATRP of MMA.*** Polymerization of MMA using the ATRP process to form PMMA brushes was previously reported by Matrab et al. (24, 31, 32) (see Scheme 1). In this study, both BrD-derived SS stents and bare stent controls (B2 stents) were inserted into two separate reactors.

Scheme 1. Schematic Illustration of the Subsequent Steps of the Stents Coating Process[a]

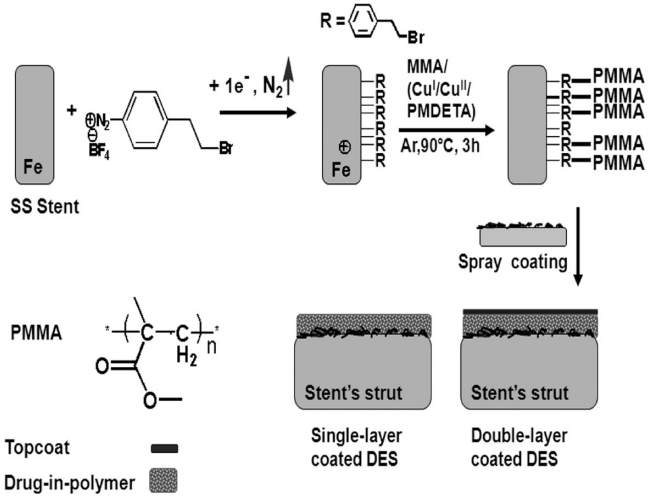

[a] In the first step, electrochemical reduction of BrD on an SS stent and then BrD-derived coating were used to initiate ATRP of MMA. The last step involved spray coating of the modified stents with a single-layer coating of PBMA/PEVA + paclitaxel or with an additional layer of PBMA (double-layer coating) to receive DESs.

Each reactor (a 50 mL two-neck flask) was deoxygenated using vacuuming and then purged with an argon gas. The flask was equipped with a magnetic stirrer and sealed with a rubber septum. Stents, 15 mg of dehydrated CuCl (15×10^{-5}mol) and 10 mg of dehydrated $CuCl_2$ (7.6×10^{-5} mol), were introduced into each working flask. MMA monomers (10 mL, 0.093 mol), PMDETA ligand (50 μL, 2.24×10^{-4} mol), and a free initiator 1-PhEtBr (65 μL, 4.49×10^{-4} mol) were injected into each working flask. The reaction was carried out under an argon atmosphere at 95 °C for a period of 3 h. The polymerization of MMA was carried out both on the surface and in the bulk and was terminated by exposing the product to air and cooling the vessel. Stents were removed from the bulk by dissolving the polymer in 50 mL of chloroform. The resulting polymeric solution was passed through a neutral alumina column to remove the copper complex. Stents (BrD and B2) were thoroughly rinsed under sonication using tetrahydrofuran, chloroform, dichloromethane, and ethanol for 15 min in each solvent. The molecular weight (M_w) of the bulk polymer was determined by gel permeation chromatography (GPC) using a Waters 1515 isocratic HPLC pump with a Waters 2410 refractive-index detector set-point temperature of 40 °C and a Rheodyne (Cotati, CA) injection valve with a 20 μL loop (Waters, Milford, MA). Samples were eluted with $CHCl_3$ through a linear Ultrastyragel column (Waters; 500 Å pore size) at a flow rate of 1 mL/min. The polymer molecular weight was calculated based on polystyrene standards (M_w of 1000−260 000 Da; Polyscience, Warrington, PA).

2.2.4. *Characterization of the Grafted Stents.* 2.2.4.1. *EIS.* EIS was performed with the electrochemical instrumentation described above (630B electrochemical analyzer, CH Instruments, Austin, TX). The working electrode was either a 316 L SS disk (0.78 cm^2), insulated in Teflon, or a stent. The stent was held by a conducting wire, and an exact volume of solution was injected into the electrochemical cell, which determined precisely the depth of the stent that was immersed into the solution. The experiment was performed at the formal potential of the $Fe(CN)_6^{3-}/Fe(CN)_6^{4-}$ couple (0.5 mM of each of the species in 0.1 M KCl) determined by cyclic voltammetry (0.23 V vs Ag/AgCl). Spectra were recorded in the frequency range of 1 Hz to 100 kHz using a 5 mV root-mean-square perturbation with 12 steps per each decade.

2.2.4.2. *XPS.* XPS measurements were performed on a Kratos Axis Ultra X-ray photoelectron spectrometer. Spectra were acquired with a monochromated Al Kα (1486.7 eV) X-ray source with a 0° takeoff angle. The pressure in the test chamber was maintained at 1.5×10^{-9} Torr during the acquisition process. The survey spectra were collected from +1200 to −5 eV (binding energy), with a pass energy of 80 eV. High-resolution XPS scans were collected for C 1s, O 1s, Fe 2p, Cr 2p, and Br 3d peaks with a pass energy of 20 eV. The step size was 1.0 eV for the survey scans and 0.1 eV for the high-resolution spectra. The XPS binding energy was calibrated with respect to the peak position of Fe^0 $2p_{3/2}$ at 707.0 eV (36). Data analysis and processing were performed with Vision Processing data reduction software (Kratos Analytical Ltd.) and CasaXPS (Casa Software Ltd.).

2.2.4.3. *Water Contact Angle.* Contact angles were evaluated using a Ramé-Hart model 100 contact-angle goniometer equipped with *Dropimage* software. Measurements were repeated three times for each sample. Each type of surface modification was studied in duplicate, and the average of all six measurements was calculated and reported.

2.2.5. *Spray Coating of Drug-in-Polymer Matrixes.* As the final coating step, stents (B2, BrD, and PMMA-BrD) were loaded with a drug-in-polymer matrix. Each tested group consisted of three stents. A designated apparatus (Sono-Tek-USA) was used to spray-coat the stents. Two solutions were used for coating the SS stents: drug-in-polymer solution I, 2% (w/v) PEVA/PBMA at a 3:7 (w/w) ratio and 1.33% (w/v) paclitaxel in ethyl acetate, and polymer solution II, 2% (w/v) PBMA in ethyl acetate.

Two types of coating models were used, double- and single-layered. In a double-layer coating model, the stent was first spray-coated with drug-in-polymer solution I and subsequently with polymer solution II as a secondary layer. In a double-layer coating, the top polymer layer (PBMA) acts as a diffusion barrier for the drug release ("slow release"). A single-layer coating was applied using the drug-in-polymer solution I without any additional diffusion barrier ("fast release"). After coating, the stents were left to dry under a gentle nitrogen flow. To ensure that the stents were not damaged in the preparation process, the coated samples were inspected using light microscopy (Zeiss). The coating weight of the samples was established using a microbalance, based on weighting of the stents before and after spraying with a drug-in-polymer matrix and drying. The spray-coating method resulted in adsorption of about 1.4 ± 0.14 $\mu g/mm^2$ paclitaxel on the stent in both types of coating models. The thickness of the drug-in-polymer coating in single-layer-coated stents was about 3 μm, while the thickness of the drug-in-polymer coating in double-layer-coated stents was about 4 μm.

Stability tests were used to evaluate the durability of the drug-in-polymer matrix and its adhesion to the stent backbone. To this end, single-layer coatings of the drug-in-polymer solution I were applied to B2, BrD, and PMMA-BrD stents. These tests were carried out in triplicate.

2.2.6. *Characterization of Drug-in-Polymer Matrixes.* The durability of the drug-in-polymer matrix was studied by comparing DESs made from B2, BrD, and PMMA-BrD stents. Single-layer-coated stents (with drug-in-polymer solution I) were incubated in a phosphate buffer (0.1 M, pH of 7.4 with 0.3% SDS) to assess the effect of incubation on the surfaces. Incubation at 37 °C was considered as exposure to physiological conditions and that at 60 °C to accelerated conditions. All tested stents were inflated at room temperature before incubation. SS stents with an initial diameter of 1.4 mm were mounted on a balloon catheter system (balloon-expandable stent system from Bx-sonic) and inflated with air to a final pressure of 10 bar (Biometrics, inflation device 200 cm^3). A final diameter of 3 mm was established.

2.2.6.1. ***SEM.*** The stents were removed from the solution, allowed to dry for 24 h, and then placed on conductive carbon paper. Samples were coated with gold to a thickness of 10 nm using a sputtering deposition machine and were imaged by a scanning electron microscope (FEI E-SEM Quanta 200) at an acceleration voltage of 30 kV.

2.2.6.2. ***Paclitaxel Controlled Release.*** DESs were prepared in triplicate using B2, BrD, and PMMA-BrD stents. The stents were coated according to "slow release" and "fast release" models, as described above. All tested DESs were inflated before incubation to a final diameter of 3 mm, as described above. Each DES was incubated in 1 mL of phosphate buffer (0.1 M, pH 7.4) with 0.3% SDS at 37 °C and rotated at 100 rpm to mimic physiological conditions (to maintain "sink conditions", 0.3% SDS was added to the phosphate buffer). Drug release was examined for more than 3 weeks, during which the buffer solution was drawn out and replaced by a fresh one at specified times. Release samples were obtained for the following 26 days. Portions of 20 μL of each sample were injected into the HPLC system (Waters, LC-Module-I). Paclitaxel was measured by reverse-phase HPLC on a C-18 column with a mobile water/ACN (45:55, v/v) phase, with the isocratic mode set to a rate of 15 min per sample (the typical retention time was ca. 7.3 min.), a flow rate of 1 mL/min, and a wavelength of 227 nm. The residual quantities of paclitaxel were extracted in chloroform and separated using an ACN/DDW (6:4, v/v) mixture, as in a previously described procedure (37).

3. RESULTS AND DISCUSSION

3.1. Electrocoating of BrD. As previously described (23), phenyldiazonium and its derivatives can be chemically attached to various conducting surfaces using chemical or electrochemical reduction. The reduction produces para-substituted phenyl radicals, a highly reactive species that tend to bind to a wide range of metals and carbonaceous materials (23). Thus, SS stents and plates were electrochemically coated with 2-bromoethylbenzene groups by cycling the potential between 0 and −1.6 V vs Ag/AgBr in the presence of BrD (Scheme 1). A broad and irreversible cathodic peak observed during the first scan disappeared in the second cycle (Figure 1), suggesting that the irreversible reduction of BrD is followed by the rapid formation of a blocking layer on the surface upon reduction of the diazonium derivative, BrD. The thickness of the organic layer formed on SS in such a reduction is on the order of a few molecular layers, that is, less than 10 nm.

The formation of a 2-bromoethylbenzene layer on the SS surface is also evident from the cyclic voltammetry of the modified electrodes in a solution of a redox couple. Figure 2 shows the cyclic voltammetry of a stent before and after BrD grafting in the presence of ferrocene. Almost complete blocking of electron transfer is attained after grafting of BrD on the SS surface.

3.2. Surface-Initiated ATRP of MMA. Grafted aryls terminated with bromide (BrD-derived stents) were used to initiate the surface polymerization of MMA and to form poly(methyl methacrylate) (PMMA) brushes. BrD-derived and bare (B2) stents were placed in separate reactors. In this process, the surface polymerization of MMA and polymerization in bulk were carried out simultaneously. At the end of the reaction, the bulk polymer (PMMA) was dissolved

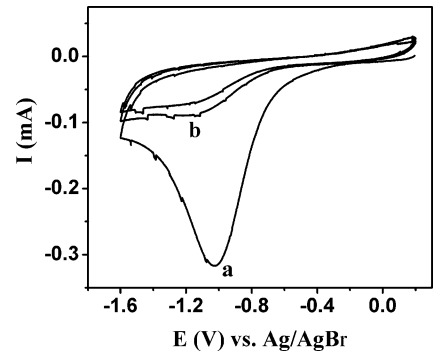

FIGURE 1. Repetitive cyclic voltammetry of 8 mM 4-bromoethylphenyldiazonium salt in 0.1 M Bu_4NF_4B in dry ACN recorded with a SS stent as a working electrode, where line a is a first scan and line b is a second scan. The scan rate was 0.1 V/s.

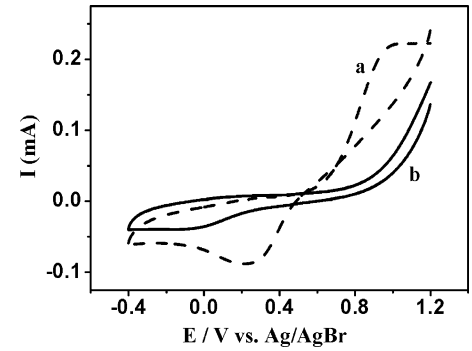

FIGURE 2. Cyclic voltammetry of 1 mM ferrocene in 0.1 M Bu_4NF_4B in dry ACN recorded with a SS stent before (a) and after (b) electrochemical reduction of 4-bromoethylphenyldiazonium salt. The scan rate was 0.1 V/s.

using chloroform. The stents were cleaned with various organic solvents to remove the physisorbed polymer chains.

3.3. PMMA Molecular Weight Analysis. The molecular weight (M_w) of bulk PMMA was measured using GPC. M_w values varied within a range of 50−65 kDa, with a polydispersity index of about 1.3. These values were determined for polymerization reactions carried out with either BrD-derived or control B2 stents. The length of the polymeric chain formed on the surface of the stents is similar to that of the bulk PMMA (24, 32). The radius of gyration, R_g, can be calculated using eq 1, where M_w is the molecular weight in Da and R_g is given in Å. R_g of the grafted PMMA is therefore about 8 nm.

$$R_g = (0.096 M_w^{0.98})^{1/2} \quad (1)$$

3.4. Characterization of the Grafted Stents. The SS surface modifications were studied using EIS, XPS, and contact-angle analysis.

3.4.1. Impedance Spectroscopy Analysis. EIS was used to determine the electrochemical characteristics of each grafting stage. Electron-transfer resistance was determined in the presence of an equimolar mixture of $Fe(CN)_6^{3-}/Fe(CN)_6^{4-}$ in a 0.1 M KCl solution. Figure 3 shows the Nyquist plot of bare SS, BrD-coated stents (BrD), PMMA grafted on a BrD layer (PMMA-BrD), and a control sample (B2). The latter is a bare SS plate that was not grafted with

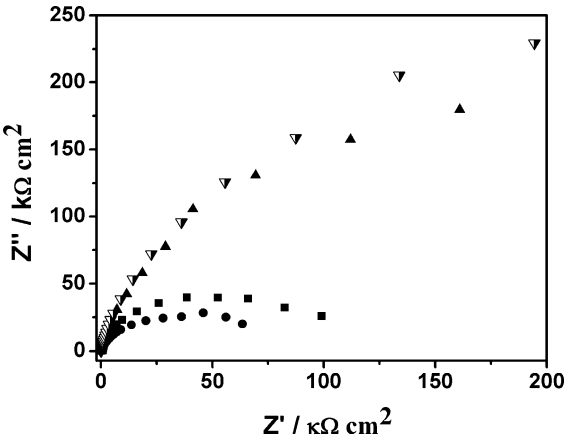

FIGURE 3. Nyquist plot of bare SS (B, ●), bare SS control after PMMA grafting (B2, ■), BrD electrocoated (▲), and PMMA coating on a BrD layer (▼) in the presence of 0.5 mM $[Fe(CN)_6]^{4-/3-}$ and 0.1 M KCl.

Scheme 2. Electrical Circuit That Was Used To Analyze the Impedance Response of the Coating[a]

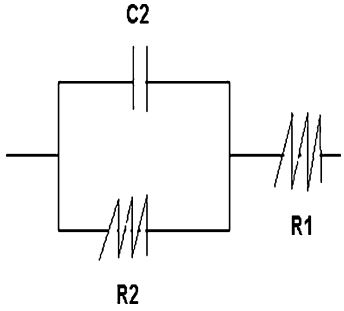

[a] R_1 and R_2 are the resistances of the solution and charge transfer, respectively, and C_2 is the coating capacity.

BrD but treated with PMMA exactly as the other samples. It is evident that the plots of the imaginary part of the impedance (Z'') versus the real part (Z') have semicirclular shape.

Therefore, the results of EIS measurements can be fit to a simple electrical circuit in which the resistance of the solution (R_1) is in series with the resistance of charge transfer (R_2) and the capacity (C_2) of the layer that are in parallel (Scheme 2).

In many cases (38), C_2 is frequency-dependent and therefore usually described as a constant phase element (CPE). Its impedance is given in eq 2, where Q is the admittance, ω is the angular frequency, j is the imaginary unit, and a is a constant describing the nature of the CPE. Specifically, when $a = 1$, the CPE is a capacitor, whereas for $a = -1$, the CPE is an inductor.

$$Z = \frac{1}{Q(j\omega)^a} \quad -1 \le a \le 1 \tag{2}$$

The total impedance can be described by eq 3:

$$Z(f) = R_1 + \frac{R_2}{R_2 Q(j\omega)^a + 1} \tag{3}$$

The data shown in Figure 3 indicate that a CPE must be taken into account. A best fit of the curves produces constant a values of 0.83 and 0.88 for the bare and modified surfaces, respectively. These values are considerably lower than those reported for a blocking layer, such as a long-chain alkanethiol on gold (39, 40), suggesting that ions are likely to penetrate the organic layer.

Table 1. Electrochemical Parameters (R_1, R_2, and C_2) Obtained from the Nyquist Plot (Figure 3)

electrochemical parameters[a]	B[b]	B2[b]	BrD[b]	PMMA-BrD[b]
R_1 (Ω/cm^2)	160	167	150	144
R_2 (Ω/cm^2)	105×10^3	164×10^3	741×10^3	1020×10^3
C_2 (μF/cm^2)	1.28	1.47	1.28×10^{-1}	1.28×10^{-2}

[a] Electrochemical parameters: R_1, resistance of the solution; R_2, charge-transfer resistance; C_2, coating capacity. [b] Acronyms: B, bare SS; B2, bare SS control after PMMA grafting; BrD, electrocoated SS; PMMA-BrD, two-step grafted SS plates.

The electrochemical parameters obtained from the Nyquist plot are presented in Table 1. The solution resistance (R_1) is relatively low because of the high concentration of KCl in the solution. R_2, obtained from curve-fitting analysis, increases with every layer. The control sample (B2) yields an R_2 value of 164 kΩ, which is greater than that produced by a bare SS (105 kΩ). It is possible that some products are formed as a result of PMMA grafting, which partly blocked electron transfer. These results are in good agreement with XPS and contact-angle analysis of the same samples.

3.4.2. XPS Analysis. Table 2 summarizes the element atomic percentage determined by XPS and data collection in high-resolution mode. The atomic values measured for bare stents (B) are in agreement with the literature (8). The absence of copper, used as the ATRP catalyst, on the surface of the stents attested to the efficiency of the stent cleaning procedure used after PMMA grafting.

The Fe 2p 710.0 eV content was highest for B2 and lowest for PMMA-BrD. The major contributors to the Fe 2p peak are the iron oxides naturally present on the SS surface. The position of the Fe 2p peak in nonorganic compounds under various coordination environments is at ca. 707.0 eV, whereas in Fe_2O_3, it was observed at 710.9 eV (36). The Fe 2p peak was moderately reduced from bare to BrD stents, and even more for PMMA-BrD stents. Detection of a Fe 2p signal at 707.0 eV on the PMMA-BrD stents indicates that

Table 2. Surface Chemical Composition of the Elements (in Atom %) in the Modified Stents Determined by XPS

	% atom[a]				
sample	Fe 2p 710−723 eV	Cr 2p 577 eV	O 1s 532 eV	C 1s 285 eV	Br 3d 70.7 eV
B[b]	0.84	2.47	48.03	47.22	
B2[b]	3.39	2.65	33.07	60.48	
BrD[b]	1.30	1.67	26.58	69.48	0.97
PMMA-BrD[b]	0.92	1.23	21.40	76.13	0.33

[a] Only the main components (Fe 2p, Cr 2p, O1s, C 1s, and Br 3d) are detailed. [b] Acronyms: B, bare stents; B2, bare stents treated with PMMA; BrD, electrocoated stents; PMMA-BrD, two-step grafted stents.

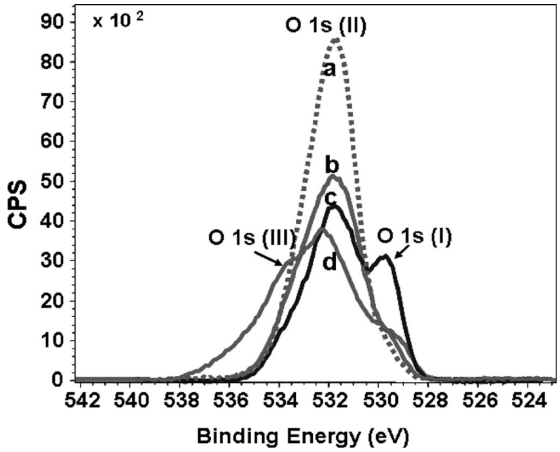

FIGURE 4. High-resolution XPS spectra of O 1s in different stents: (a) B control stent, (b) BrD electrochemically treated stent, (c) B2 control stent; (d) two-step grafted stent PMMA-BrD.

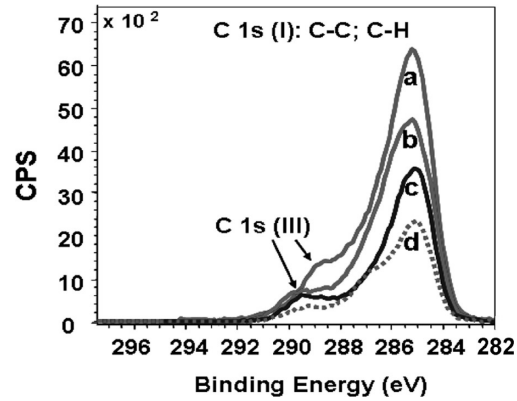

FIGURE 6. High-resolution XPS spectra of C 1s in different stents: (a) two-step grafted stent PMMA-BrD, (b) BrD electrochemically treated stent, and (c) B2 and (d) B control stents.

coverage by the polymer brushes is incomplete or that the thickness of the coating is lower than about 10 nm. The Cr 2p content profile was similar to that of Fe 2p. Again, Cr 2p was detected least in the PMMA-BrD stents. The Cr 2p originates from Cr_2O_3, and its position is 576.9 eV (36). The SS is naturally coated with a layer of metallic oxides (mainly Cr_2O_3) of thicknesses of about 10−50 Å (8).

The percentage of coverage cannot be calculated directly from the XPS data and therefore can only be a qualitative measure of the density of coverage. The atomic percent of iron and chromium decreased by more than 30% (from 4.31% to 2.97%), yet it only means that the multilayer of BrD that is formed is not dense and therefore does not totally attenuate the ejected electrons coming from the surface.

The presence of the PMMA brushes was supported by the collection of high-resolution spectra of O 1s and C 1s. These peaks changed significantly after BrD and PMMA grafting (see Figures 4−7).

The oxygen concentration in bare stents was highest because of the thick oxide layer (~50 Å) (8), and it constituted 100% of the peak at 531.7 eV. Similarly, B2 and BrD stents revealed 100% of inorganic oxygen, probably from metallic hydroxide oxides (41). A significant difference in the oxygen signal was detected between the diazonium-coated stent, BrD, and the two-step grafted stent (PMMA-BrD), where for PMMA-BrD 71.4% of the oxygen peak shifted to 533.4 eV. This shift to higher energy (533.4 eV) alludes to an organic oxygen neighborhood that originates with the ester groups (−COO−) in PMMA brushes and not with the typical inorganic oxides of SS (42, 43). Inorganic oxygen originating with iron(III) oxide (529.7 eV) (32) and chromium(III) oxide (529.9 eV) (44) was present in all three systems (Figures 4 and 5). It appears, therefore, that surface pretreatment by electrochemical reduction was not complete.

Similarly, C 1s peak (285−289.3 eV) components varied between bare, BrD-derived, and BrD-PMMA stents (Figures 6 and 7). These changes can again be attributed to the formation of the PMMA brushes. For PMMA-BrD stents, the C 1s peak (III) appeared at 289.3 eV, which can be attributed to the ester bond in the PMMA-grafted layer (31, 32, 45).

The contribution of the −*C*OO− peak (289.3 eV) to the total carbon atomic concentration intensified from 9.4% at the bare stent to 13.4% at the BrD stent and to 22.8% for the PMMA-BrD stent. Furthermore, the total percentage of carbon contributions increased from 69.5% to 76.1% for the BrD- and PMMA-BrD-modified stents and was 47.2% for the bare stents.

The data derived from XPS analysis confirmed the presence of a (2-bromoethyl)benzene layer on stents and the

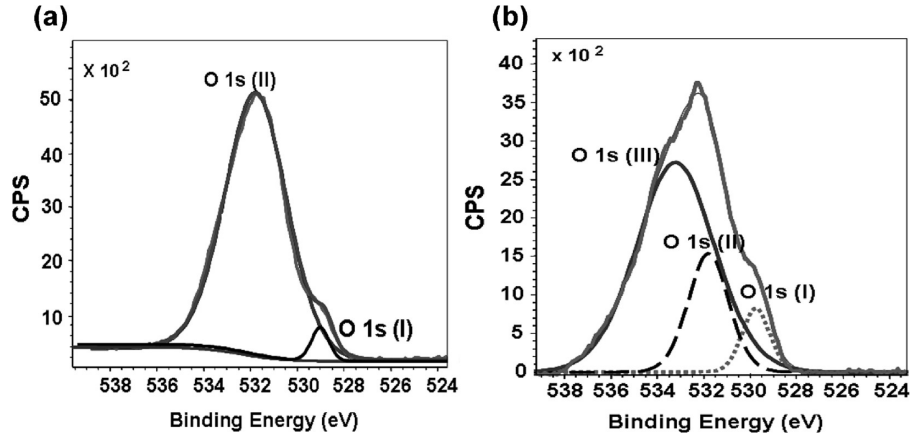

FIGURE 5. High-resolution O 1s peak composition of (a) the diazonium electrocoated stent BrD and (b) the two-step grafted stent PMMA-BrD.

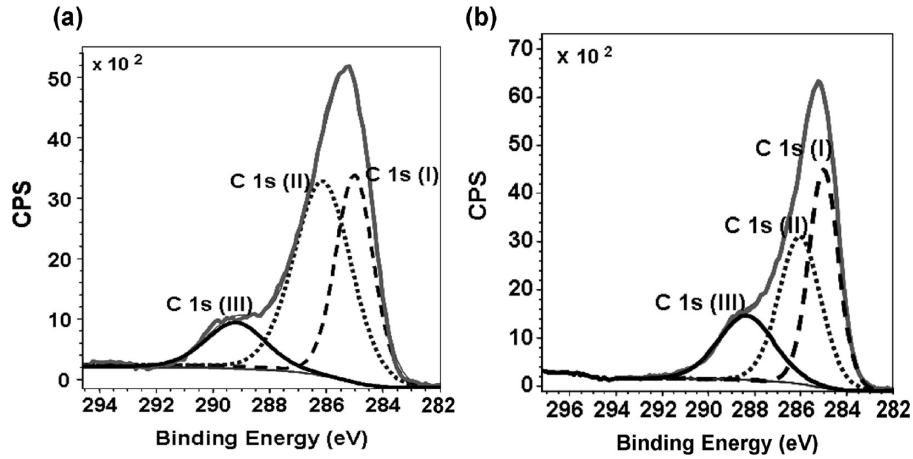

FIGURE 7. High-resolution XPS spectra of the C 1s peak of (a) the diazonium electrocoated stent BrD and (b) the two-step grafted stent PMMA-BrD.

further formation of PMMA brushes on this primer layer. It also appears that coverage by the polymer brushes was not homogeneous and its thickness was lower than about 10 nm.

3.4.3. Water Contact-Angle Analysis. The water contact-angle value measured on SS plates was 62 ± 2.8°. Contact-angle measurements, performed using B2, BrD-derived, and BrD-PMMA plates, produced typical values of 72.4 ± 3.2°, 85.1 ± 7.1°, and 71.8 ± 2.1°, respectively. These data provide a direct indication of the success of various grafting procedures. The literature contact-angle value for PMMA sheets is 64° (31). The higher measured value may be attributed to the primer aryl layer, which enhances the hydrophobicity of the surface, or to an incomplete coverage of the PMMA brushes. The contact angle for the drug-in-polymer matrix (7:3 PBMA/PEVA with paclitaxel in a 6:4 ratio) on SS was 84.6 ± 1.6°, while the contact angle without the drug was somewhat higher, 87.7 ± 0.8°.

3.5. Characterization of Drug-in-Polymer Matrixes. Control (B2), BrD-derived, and PMMA-BrD stents were spray-coated with a drug-in-polymer matrix using a designated spray-coating machine (Medicoat; Sonotek, USA). DESs were inflated to a nominal diameter of 3 mm. At zero time, stent coatings were highly flexible and the inflated stent coatings showed no detectable cracking or delamination (data not shown, similar to Figure 8a,b). Accordingly, the durability of the coating was further studied after DES incubation in either physiological (37 °C) or accelerated (60 °C) conditions (phosphate buffer, 0.1 M, pH 7.4, 0.3% SDS 100 rpm; Figures 9 and 10). Following the incubation period, samples were pulled from the buffer, dried at room temperature, and tested using SEM and light microscopy.

3.5.1. Stent Coating Durability after Incubation in a Physiological Buffer. Control (B2), BrD-derived, and PMMA-BrD stents were spray-coated with a drug-in-polymer matrix according to the single-layer model [paclitaxel-in-(PBMA/PEVA) matrix; paclitaxel loading of about 1.4 ± 0.14 μg/mm^2].

Figure 9 shows SEM images for these stents after 3 days of incubation in a phosphate buffer (0.1 M, pH 7.4) at 60 °C and under continuous stirring at 100 rpm. Single-layer

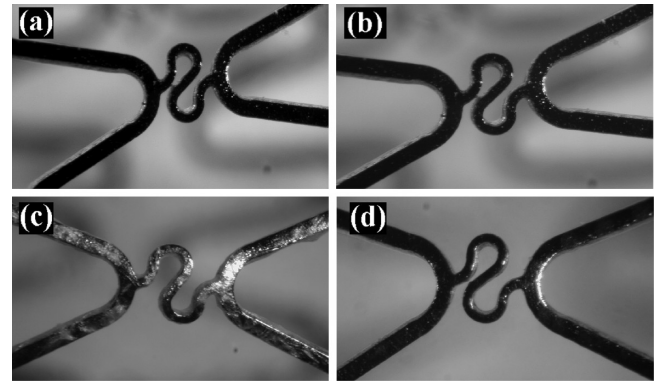

FIGURE 8. Light microscope images of stents loaded with a drug-in-polymer matrix and a polymer top-coat (double-layer coating), inflated to a final open diameter of 3 mm: (a) B2 stents' and (b) PMMA-BrD stents' struts. The stents were photographed after 2 weeks of drug release (incubation in a phosphate buffer of 0.1 M, pH 7.4, 0.3% SDS at 37 °C, 100 rpm). (c) B2 control stent coating which delaminated and became white. (d) PMMA-BrD showing almost unaltered morphology of the polymer coating.

coatings of a drug-in-polymer matrix on both bare control (B2) and electrocoated (BrD) stents showed significant pealing and delamination (Figure 9a,b,d,e). However, the drug-in-polymer coating on PMMA-BrD DESs remained unaltered (see Figure 9c,f). Light microscopy images show that the delaminated coating became white (light reflection as a result of delaminated polymer layers from the metal and buffer diffusion into the porous matrix). By contrast, the coatings of PMMA-BrD-treated stents behaved similarly to zero-time samples (data not shown, similar to Figure 8c,d).

Similar results were obtained for the single-layer-coated DESs ("fast release model") incubated under physiological conditions for 3 days (see Figure 10). B2 metal struts suffered from poor adhesion to the drug-in-polymer matrix, wide areas of polymer were detached from the stent backbone, and the metal surface was exposed (Figure 10a,c). The PMMA-BrD stents showed a uniform polymer surface, on which only the drug was released (Figure 10b,d).

Figure 11 shows SEM images of DESs after 14 days of incubation at physiological conditions. In this study, control (B2), BrD-derived, and PMMA-BrD stents were spray-coated according to the double-layer model ("slow release"). First,

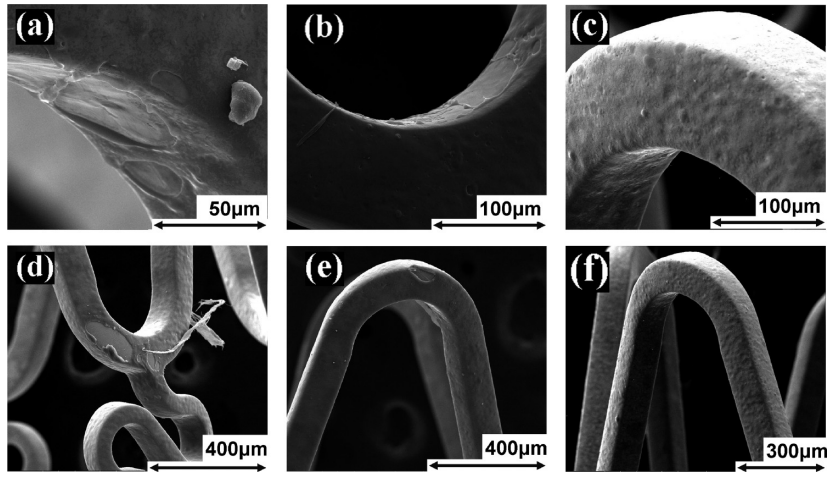

FIGURE 9. Comparison of a paclitaxel-in-(PBMA/PEVA) coating on bare B2, BrD, and PMMA-BrD stents. SEM visualization of the polymer coating was done with DESs after incubation under accelerated conditions for 3 days: (a and d) bare stent B2; (b and e) diazonium-electrocoated BrD; (c and f) two-step grafted PMMA-BrD. Accelerated conditions: phosphate buffer, 0.1 M, pH 7.4, 0.3% SDS at 60 °C, 100 rpm.

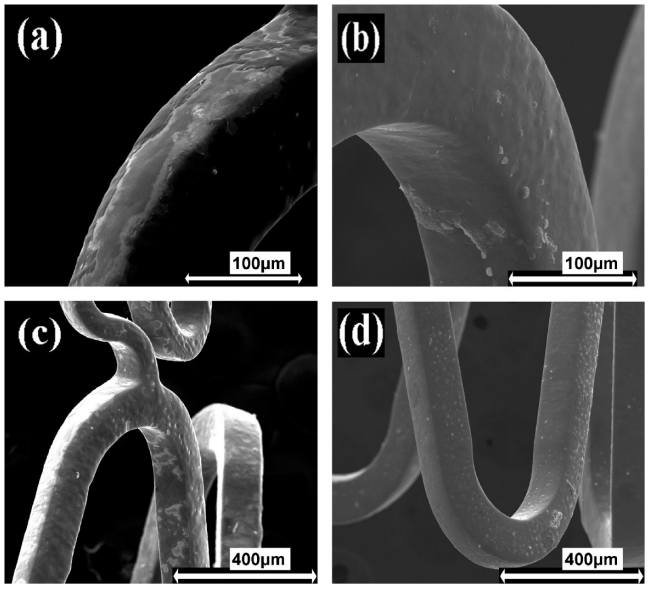

FIGURE 10. SEM images of B2 stents (a and c) and PMMA-BrD stents (b and d) coated with a single layer of the drug-in-polymer matrix and then incubated under physiological conditions for 3 days (phosphate buffer, 0.1 M, pH 7.4, 0.3% SDS at 37 °C, 100 rpm).

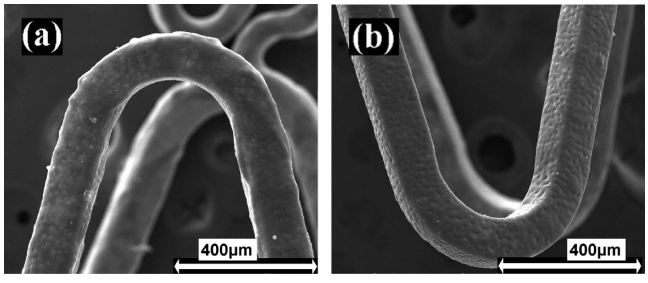

FIGURE 11. SEM images following 14 days of incubation under physiological conditions of double-layer-coated DESs. Bare (B2) stents (a) and two-step grafted (PMMA-BrD) stents (b) were loaded with paclitaxel-in-(PBMA/PEVA) and additional polymer top coat (PBMA) and then incubated under physiological conditions for 14 days (phosphate buffer, 0.1 M, pH 7.4, 0.3% SDS at 37 °C, 100 rpm).

the paclitaxel-in-(PBMA/PEVA) matrix was applied, resulting in a drug distribution of about $1.4 \pm 0.14\ \mu g/mm^2$; next, an additional top coat of PBMA was applied. The coating of these DESs showed no significant cracking or delamination for either the control or the modified group, but the light microscopy images of the drug-in-polymer coatings on B2 DESs appeared white because of delamination and buffer diffusion into the already porous inner layers of the polymer (Figure 8c). BrD-derived and PBMA-BrD DESs drug-in-polymer matrixes generally preserved their original morphology (Figure 8d).

3.5.2. Controlled Release of Paclitaxel. Durability studies carried out under both accelerated and physiological conditions demonstrated that PMMA-grafted brushes substantially enhanced the stability of the drug-in-polymer matrix. It was, therefore, important to study whether these differences also affected the main functional requirement of DESs, which is to release an antirestenotic agent in a controlled manner. SS stents (B2, BrD, and PMMA-BrD) were spray-coated with either a single- or a double-layer coating. The drug content was $1.44 \pm 0.05\ \mu g/mm^2$ for B2 stents, $1.40 \pm 0.12\ \mu g/mm^2$ for BrD stents, and $1.40 \pm 0.13\ \mu g/mm^2$ for PMMA-BrD stents.

Figure 12 shows the cumulative paclitaxel release profile in vitro from the spray-coated DESs. A significant change was observed in the release pattern between BrD and B2 stents, which were spray-coated with a single layer, and the drug release rate increased gradually between the two tested groups. BrD-derived and bare control (B2) stents had initial bursts of 52% and 64.5%, respectively, after 1 day. Similar trends were observed for double-layer-coated stents, where the secondary polymer coating (PBMA) was responsible for the moderate drug release. The PMMA-BrD, BrD, and B2 DESs were characterized by initial bursts of 20.8, 31.8, and 34%, respectively, at 1 day. After 14 days in a physiological buffer, PMMA-BrD DESs released less than 60% of the drug, whereas B2 DESs released almost 80% of the initial drug load.

In the last study, we observed again the beneficial effects of introducing a thin organic layer as the interface between the rather hydrophilic SS (with a water contact angle of ca. 62°) and the hydrophobic drug-in-polymer

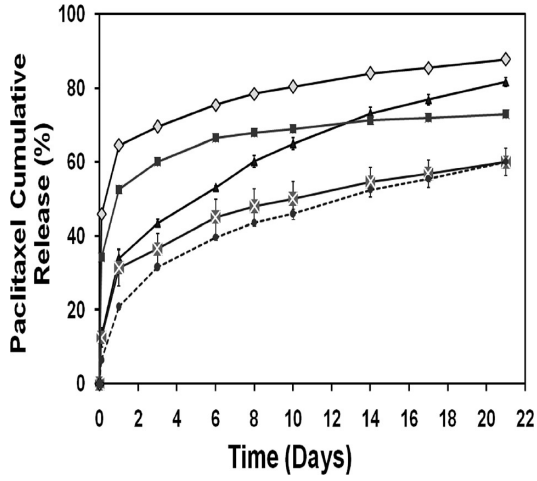

FIGURE 12. In vitro cumulative paclitaxel release profile from different DESs for a period of 3 weeks. A "fast release profile" was obtained for the B2 stents (gray ◊) and for BrD stents (■) coated with a single layer of the drug-in-polymer matrix [paclitaxel-in-(PBMA/PEVA)]. A "slower release profile" was obtained for the B2 stents (▲), BrD stents (⊠), and PMMA-BrD stents (●) coated with the drug-in-polymer matrix and additional polymer top coat (PBMA).

matrix (with a water contact angle of ca. 85°). The enhanced durability and stability of the drug-in-polymer matrix had a gradual effect on the drug release characteristics of the BrD and PMMA-BrD DESs. Both organic layers, BrD and PMMA-BrD, showed the beneficial effects for the DESs. However, the effect was intensified by the PMMA-BrD layer, possibly as a result of the similar chemical structure of PMMA brushes and the drug-carrying polymer PBMA. This may also indicate that a more significant SS surface coverage is desirable than that achieved by a thin layer of BrD. Similar results were obtained in parallel work performed by our research group, in which the surface was modified with an aromatic diazonium salt with a long aliphatic chain, 4-(1-dodecyloxy)-phenyldiazonium tetrafluoroborate (29).

4. CONCLUSIONS

SS stents were electrochemically modified with a layer of 4-(2-bromoethyl)benzenediazonium salt, which served as a radical initiator for further ATRP of MMA. XPS and electrochemical analysis confirmed the formation of a uniform organic coating. This covalently attached layer significantly improved the drug-in-polymer matrix adhesion to the SS stent backbone. Durability of the drug-in-polymer coatings was demonstrated through stability testing under physiological and accelerated conditions. Paclitaxel controlled release from the modified SS DESs demonstrated a moderate profile relative to nontreated samples. It is clear, therefore, that the PMMA-BrD layer substantially improved the durability of the polymer/drug-in-polymer matrix on SS stents.

Acknowledgment. This work was supported in part by an Israel Science Foundation grant, to which the authors are grateful. The unit for Nanocharacterization of Hebrew University is acknowledged.

REFERENCES AND NOTES

(1) Burt, H. M.; Hunter, W. L. *Adv. Drug Delivery Rev.* **2006**, *58*, 350–357.
(2) Rogers, C. D. *Rev. Cardiovasc. Med.* **2004**, *5* (2), S9–S15.
(3) U.S. Food and Drug Administration, Center for Devices and Radiological Health, "CYPHER Sirolimus-eluting coronary stent—P020026". Available from http://www.fda.gov/MedicalDevices/ProductsandMedicalProcedures/DeviceApprovalsandClearances/Recently-ApprovedDevices/ucm082499.htm, updated June 6, 2009.
(4) Ranade, S. V.; Miller, K. M.; Richard, R. E.; Chan, A. K.; Allen, M. J.; Helmus, M. N. *J. Biomed. Mater. Res., Part A* **2004**, *71*, 625–634.
(5) Kereiakes, D. J.; Cox, D. A.; Hermiller, J. B.; Midei, M. G.; Bachinsky, W. B.; Nukta, E. D.; Leon, M. B.; Fink, S.; Marin, L.; Lansky, A. J. *Am. J. Cardiol.* **2003**, *92*, 463–466.
(6) Pelton, A. R.; Schroeder, V.; Mitchell, M. R.; Gong, X. Y.; Barney, M.; Robertson, S. W. *J. Mech. Behav. Biomed. Mater.* **2008**, *1*, 153–164.
(7) Mani, G.; Feldman, M. D.; Patel, D.; Agrawal, C. M. *Biomaterials* **2007**, *28*, 1689–1710.
(8) Haidopoulos, M.; Turgeon, S.; Sarra-Bournet, C.; Laroche, G.; Mantovani, D. *J. Mater. Sci.: Mater. Med.* **2006**, *17*, 647–657.
(9) Adams, R. O. *J. Vac. Sci. Technol., Part A* **1983**, *1*, 12–18.
(10) Istephanous, N.; Bai, Z.; Gilbert, J. L.; Rohly, K.; Belu, A.; Trausch, I.; Untereker, D. Oxide films on metallic biomaterials: Myths, facts and opportunities. *Thermec'2003*; Trans Tech Publications: Stafa-Zurich, Switzerland, 2003; Vol. 426-4, pp 3157—3163.
(11) Lee, Y. K.; Hyung Park, J.; Tae Moon, H.; Yun Lee, D.; Han Yun, J.; Byun, Y. *Biomaterials* **2007**, *28*, 1523–1530.
(12) Lewis, A. L.; Vick, T. A.; Collias, A. C.; Hughes, L. G.; Palmer, R. R.; Leppard, S. W.; Furze, J. D.; Taylor, A. S.; Stratford, P. W. *J. Mater. Sci.: Mater. Med.* **2001**, *12*, 865–870.
(13) Lewis, A. L.; Willis, S. L.; Small, S. A.; Hunt, S. R.; O'Byrne, V.; Stratford, P. W. *Biomed. Mater. Eng.* **2004**, *14*, 355–370.
(14) Venkatraman, S.; Boey, F. *J. Controlled Release* **2007**, *120*, 149–160.
(15) Finkelstein, A.; McClean, D.; Kar, S.; Takizawa, K.; Varghese, K.; Baek, N.; Park, K.; Fishbein, M. C.; Makkar, R.; Litvack, F.; Eigler, N. L. *Circulation* **2003**, *107*, 777–784.
(16) Pan, C. J.; Shao, Z. Y.; Tang, J. J.; Wang, J.; Huang, N. *J. Biomed. Mater. Res., Part A* **2007**, *82*, 740–746.
(17) Sousa, J. E.; Serruys, P. W.; Costa, M. A. *Circulation* **2003**, *107*, 2274–2279.
(18) Gershlick, A. H. *Heart* **2005**, *91* (3), iii24–31.
(19) Virmani, R.; Guagliumi, G.; Farb, A.; Musumeci, G.; Grieco, N.; Motta, T.; Mihalcsik, L.; Tespili, M.; Valsecchi, O.; Kolodgie, F. D. *Circulation* **2004**, *109*, 701–705.
(20) Nakazawa, G.; Finn, A. V.; Kolodgie, F. D.; Virmani, R. *Expert Rev. Med. Devices* **2009**, *6*, 33–42.
(21) Windecker, S.; Meier, B. *Circulation* **2007**, *116*, 1952–1965.
(22) Otsuka, Y.; Chronos, N. A.; Apkarian, R. P.; Robinson, K. A. *J. Invasive Cardiol.* **2007**, *19*, 71–76.
(23) Pinson, J.; Podvorica, F. *Chem. Soc. Rev.* **2005**, *34*, 429–439.
(24) Matrab, T.; Chancolon, J.; L'Hermite, M. M.; Rouzaud, J. N.; Deniau, G.; Boudou, J. P.; Chehimi, M. M.; Delamar, M. *Colloids Surf., Part A* **2006**, *287*, 217–221.
(25) Palacin, S.; Bureau, C.; Charlier, J.; Deniau, G.; Mouanda, B.; Viel, P. *ChemPhysChem* **2004**, *5*, 1469–1481.
(26) Adenier, A.; Cabet-Deliry, E.; Lalot, T.; Pinson, J.; Podvorica, F. *Chem. Mater.* **2002**, *14*, 4576–4585.
(27) Adenier, A.; Bernard, M. C.; Chehimi, M. M.; Cabet-Deliry, E.; Desbat, B.; Fagebaume, O.; Pinson, J.; Podvorica, F. *J. Am. Chem. Soc.* **2001**, *123*, 4541–4549.
(28) Hurley, B. L.; McCreery, R. L. *J. Electrochem. Soc.* **2004**, *151*, B252–B259.
(29) Levy, Y.; Tal, N.; Weinberger, N. T. J.; Domb, A. J.; Mandler, D. *J. Biomed. Mater. Res., Part B* **2009**, *21B*, 819–830.
(30) Rakhmatullina, E.; Braun, T.; Kaufmann, T.; Spillmann, H.; Malinova, V.; Meier, W. *Macromol. Chem. Phys.* **2007**, *208*, 1283–1293.
(31) Matrab, T.; Chehimi, M. M.; Perruchot, C.; Adenier, A.; Guillez, A.; Save, M.; Charleux, B.; Cabet-Deliry, E.; Pinson, J. *Langmuir* **2005**, *21*, 4686–4694.

(32) Matrab, T.; Save, M.; Charleux, B.; Pinson, J.; Cabet-Deliry, E.; Adenier, A.; Chehimi, M. M.; Delamar, M. *Surf. Sci.* **2007**, *601*, 2357–2366.
(33) Haas, S. S.; Brauer, G. M.; Dickson, G. *J. Bone Joint Surg. Am.* **1975**, *57*, 380–391.
(34) Mousa, W. F.; Kobayashi, M.; Shinzato, S.; Kamimura, M.; Neo, M.; Yoshihara, S.; Nakamura, T. *Biomaterials* **2000**, *21*, 2137–2146.
(35) Ruan, C. M.; Bayer, T.; Meth, S.; Sukenik, C. N. *Thin Solid Films* **2002**, *419*, 95–104.
(36) Moulder, J. F.; Stickle, W. F.; Sobol, P. E.; Bomben, K. D. In *Handbook of X-ray Photoelectron Spectroscopy*, 2nd ed.; Chastain, J., Ed.; Physical Electronics Division, Perkin-Elmer Corp.: Eden Prairie, MN, 1992.
(37) Okner, R.; Shaulov, Y.; Tal, N.; Favaro, G.; Domb, A. J.; Mandler, D. *ACS Appl. Mater. Interfaces* **2009**, *1*, 758–767.
(38) Kendig, M.; Scully, J. *Corrosion* **1990**, *46*, 22–29.
(39) Diao, P.; Jiang, D. L.; Cui, X. L.; Gu, D. P.; Tong, R. T.; Zhong, B. *J. Electroanal. Chem.* **1999**, *464*, 61–67.
(40) Janek, R. P.; Fawcett, W. R.; Ulman, A. *Langmuir* **1998**, *14*, 3011–3018.
(41) Allen, G. C.; Curtis, M. T.; Hooper, A. J.; Tucker, P. M. *J. Chem. Soc., Dalton Trans.* **1974**, 1525–1530.
(42) Beamson, G.; Briggs, D. *High Resolution XPS of Organic Polymers: The Scienta ESCA300 Database*; John Wiley & Sons Inc.: Chichester, England, 1992.
(43) Burrell, M. C.; Liu, Y. S.; Cole, H. S. *J. Vac. Sci. Technol.* **1986**, *A4*, 2459.
(44) Dickinson, T.; Povey, A. F.; Sherwood, P. M. A. *J. Chem. Soc., Faraday Trans. 1* **1976**, *72*, 686–705.
(45) Zhang, F.; Kang, E. T.; Neoh, K. G.; Wang, P.; Tan, K. L. *Biomaterials* **2001**, *22*, 1541–1548.

AM900465T